



# Microwave properties of $BaFe_{11}Mg_{0.25}^{2+}X_{0.25}^{2+}Ti_{0.25}^{4+}O_{19}$ ( $X^{2+} = Cu, Mn, Zn, Ni$ and $Co$ ) nanoparticles in 0–26.5 GHz range

H. Sözeri<sup>a,\*</sup>, Z. Mehmedi<sup>a</sup>, H. Erdemi<sup>b</sup>, A. Baykal<sup>c</sup>, U. Topal<sup>a</sup>, B. Aktaş<sup>d</sup>

<sup>a</sup>TUBITAK-UME, National Metrology Institute, PO Box 54, 41470 Gebze-Kocaeli, Turkey

<sup>b</sup>Yalova University, Department of Polymer Engineering, 77100 Yalova, Turkey

<sup>c</sup>Fatih University, Chemistry Department, 34500 B.Çekmece-İstanbul, Turkey

<sup>d</sup>Department of Physics, Gebze Technical University, P.B. 141, Gebze, Kocaeli 41400, Turkey

Received 11 September 2015; received in revised form 8 October 2015; accepted 13 October 2015

Available online 18 October 2015

## Abstract

The structural, magnetic and microwave properties of cation substituted barium hexaferrite nanoparticles were investigated. Samples having composition of  $BaFe_{11}Mg_{0.25}^{2+}X_{0.25}^{2+}Ti_{0.25}^{4+}O_{19}$  ( $X^{2+} = Cu, Mn, Zn, Ni$  and  $Co$ ) were synthesized with solid state reaction route and 1 wt% boron was added as a catalyst to initialize the crystal growth. XRD analysis showed that hard hexaferrite phase was successfully obtained. The lattice parameters “*a*” and “*c*” are almost the same in all substituted ions except  $Cu^{2+}$ , in which elongation in *c*-axis was detected. The highest saturation magnetization occurred in  $Ni^{2+}$  and the highest coercivity was observed in  $Cu^{2+}$  substituted samples. This was explained by site preferences of cations which has direct influence on strength of Fe–O–Fe superexchange interactions. The both ac ( $\sigma_{ac}$ ) and dc ( $\sigma_{dc}$ ) conductivities have temperature dependency and vary with substitution of  $Cu^{2+}$ ,  $Zn^{2+}$ ,  $Co^{2+}$ ,  $Mn^{2+}$  and  $Ni^{2+}$  ions. The maximum ac conductivity was observed as  $2.39 \times 10^{-6} \text{ S cm}^{-1}$  in  $Ni^{2+}$  substituted sample at 120 °C and at 10 Hz. The increase in dielectric constants ( $\epsilon'$ ,  $\epsilon''$ ) with variation of substituted divalent ions was explained by reduction of electron hopping between  $Fe^{2+}$  and  $Fe^{3+}$  ions. The absorption of incident microwave occurs at two different frequencies, around 10 and 20 GHz. The reflection loss close to 10 GHz was observed in all samples, whereas Mn, Zn and Ni substituted samples have the secondary reflection minima. The mechanism of reflection loss at low frequency is quarter wave cancellation at matching thickness. And, at high frequency, it is due to the natural resonance and dipole relaxation of fillers. The best absorption capability was obtained in  $Mn^{2+}$  substituted sample, which has reflection losses of  $-30$  and  $-29$  dB at 9.5 and 19.2 GHz. © 2015 Elsevier Ltd and Techna Group S.r.l. All rights reserved.

**Keywords:** Nanostructured materials; Solid state reaction; Microwave properties; Magnetic measurements; Cation substitution

## 1. Introduction

The widespread usage of wireless communication systems like mobile phones, local area networks and radar systems created the new type pollution, namely an electromagnetic interference, which can be partially overcome by using microwave absorbing materials. There has been increasing interest in development of such materials which have wide band and strong absorption properties together with features like low density and low cost [1].

In microwave absorbers, magnetic and dielectric fillers are used to diminish both electric and magnetic field components of incident wave [1–3]. As magnetic fillers, ferrites both spinel and hexaferrites are frequently used to damp energy of incoming microwave by domain wall motions and spin rotation mechanisms. Among hexaferrites, barium hexaferrite (BaM) has been studied extensively due its excellent chemical stability, high saturation magnetization and high magnetocrystalline anisotropy, good dielectric properties, low cost and observation of ferromagnetic resonance in microwave band [4–8].

The absorption of an incident microwave occurs when two conditions are satisfied. The first, electromagnetic wave should easily penetrate the material, which can be done by matching the impedance of air and the absorber. When this condition is

\*Corresponding author. Tel.: +90 262 679 5000; fax: +90 262 679 5001.

E-mail address: [huseyin.sozeri@tubitak.gov.tr](mailto:huseyin.sozeri@tubitak.gov.tr) (H. Sözeri).

satisfied incoming wave penetrates into the material completely. Secondly, material should have lossy fillers which convert electromagnetic energy to the heat through several dissipation mechanisms like conduction, resonance or relaxation. The complex parts of the permittivity and permeability of material plays crucial role in this process. In order to improve magnetic and microwave properties of magnetic fillers (i.e. hexaferrites in this case), divalent, divalent–tetravalent, trivalent cationic substitutions for  $\text{Fe}^{3+}$  ion have been studied [9–11].

In this study, one  $\text{Fe}^{3+}$  ion was replaced by  $\text{Mg}^{2+}$ ,  $\text{Ti}^{4+}$  and one of the  $\text{Co}^{2+}$ ,  $\text{Mn}^{2+}$ ,  $\text{Zn}^{2+}$ ,  $\text{Ni}^{2+}$ ,  $\text{Cu}^{2+}$  ions. BaM samples in the form of  $\text{BaFe}_{11}\text{Mg}_{0.25}\text{X}_{0.25}\text{Ti}_{0.5}\text{O}_{19}$  ( $\text{X}^{2+} = \text{Co}^{2+}$ ,  $\text{Mn}^{2+}$ ,  $\text{Zn}^{2+}$ ,  $\text{Ni}^{2+}$ , and  $\text{Cu}^{2+}$ ) were synthesized with conventional solid state reaction route. The structural, magnetic and microwave properties of samples were investigated by X-ray diffractometry, scanning electron microscopy, room temperature magnetization measurements and transmission/reflection measurements in network analyzer in 0–26.5 GHz range. Reflection losses were calculated from the S-parameters using NRW algorithm. Microwave properties of samples having various thicknesses were also determined.

## 2. Experimental

Following reagent chemicals were used to synthesize  $\text{BaFe}_{11}\text{Mg}_{0.25}\text{X}_{0.25}\text{Ti}_{0.5}\text{O}_{19}$  ( $\text{X} = \text{Mn}$ ,  $\text{Co}$ ,  $\text{Ni}$ ,  $\text{Cu}$ , and  $\text{Zn}$ );  $\text{BaCO}_3$ ,  $\text{Fe}_2\text{O}_3$ ,  $\text{MgO}$ ,  $\text{XO}$ ,  $\text{TiO}_2$ ,  $\text{B}_2\text{O}_3$  and ethanol were purchased from Merck and were used without further purification. For the solid state reaction of X (Mn, Co, Ni, Cu, and Zn),  $\text{BaCO}_3$ ,  $\text{Fe}_2\text{O}_3$  and  $\text{B}_2\text{O}_3$  to form  $\text{BaMg}_{0.25}\text{X}_{0.25}\text{Ti}_{0.5}\text{Fe}_{11}\text{O}_{19}$ , ingredients were weighted stoichiometrically and  $\text{B}_2\text{O}_3$  1 wt% was added. Then, the precursor were grounded and grinded in an agate mortar together, first in solid phase, then in ethanol medium for 15 min. The mixture was pelletized under 200 MPa pressure, which were heat treated at temperature 1000 °C for 2 h. After the heat treatment, toroidal and rectangular pellets were prepared for microwave characterization of the samples. The magnetic characterization of all samples was performed at room temperature using a vibrating sample magnetometer (LDJ Electronics Inc. Model 9600) in an applied field of 15 kOe. The microwave measurements, were performed in Reflection/Transmission mode in a coaxial airline using HP PNA E8364B vector network analyzer in the frequency range of 2–18 GHz and in 18–26.5 GHz in waveguide. The material measurement software was used to derive complex permeability and permittivity values from the measured transmission ( $S_{21}$ ) and reflection ( $S_{11}$ ) coefficients.

## 3. Results and discussion

### 3.1. XRD analysis

The XRD powder patterns of the products are shown in Fig. 1. Refinement of all the patterns was performed via Rietveld method to obtain the best fit index up to one. Sharp, intense and characteristic peaks are easily observed in Fig. 1. Structural parameters derived from the XRD data analyses are given in

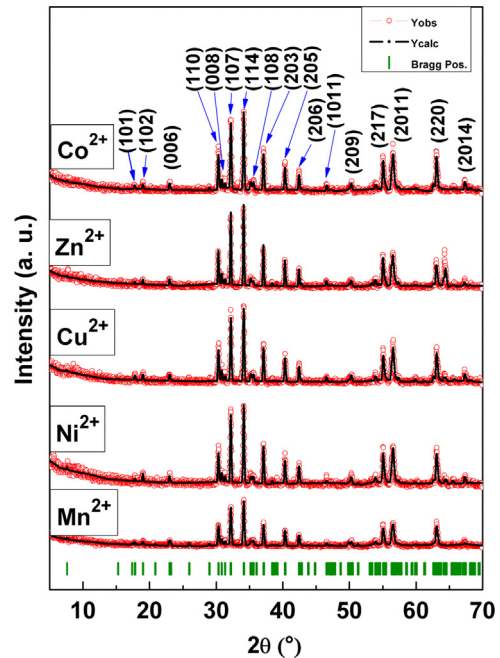


Fig. 1. XRD spectra with Rietveld analysis patterns for  $\text{BaFe}_{11}\text{Mg}_{0.25}\text{X}_{0.25}\text{Ti}_{0.5}\text{O}_{19}$  nanoparticles (NPs).

Table 1

Lattice parameters and Crystal sizes of  $\text{BaFe}_{11}\text{Mg}_{0.25}\text{X}_{0.25}\text{Ti}_{0.5}\text{O}_{19}$  ( $\text{X} = \text{Co}$ ,  $\text{Cu}$ ,  $\text{Ni}$ ,  $\text{Zn}$ ,  $\text{Mn}$ ) NPs calculated by Scherrer's formula from the (114) peak.

Sample	$a=b$ (Å)	$c$ (Å)	Crystallite size (nm)
BaM [12]	5.892001	23.183001	–
$\text{Mn}^{2+}$	5.891518	23.212355	39.14
$\text{Co}^{2+}$	5.892155	23.204216	41.10
$\text{Ni}^{2+}$	5.891612	23.211765	39.13
$\text{Cu}^{2+}$	5.890830	23.204382	43.26
$\text{Zn}^{2+}$	5.894251	23.213785	45.71

Table 1. Rietveld analysis of the XRD powder patterns shows the formation of single phase hexagonal ferrites (space group P63/mmc, JCPDS file number 84-0757). No secondary phase is observed from the XRD patterns.

Table 1 depicts that lattice constants  $a$  and  $c$ , the  $c/a$  ratio, and the cell volume  $V$  change with ionic substitution. These variations can mainly be explained on the basis of the ionic radius of the substituted ions. The ionic radii of  $\text{Co}^{2+}$ ,  $\text{Ni}^{2+}$ ,  $\text{Mn}^{2+}$ ,  $\text{Zn}^{2+}$ ,  $\text{Cu}^{2+}$ , and  $\text{Fe}^{3+}$ , are 0.79, 0.83, 0.81, 0.88, and 0.87 Å respectively, and larger than that of  $\text{Fe}^{3+}$  (0.69 Å). Similar results were reported for polycrystalline  $\text{BaFe}_{12}\text{O}_{19}$  system [12,13]. Hence, the variation of lattice parameters and grain size indicates that  $\text{Co}^{2+}$ ,  $\text{Ni}^{2+}$ ,  $\text{Mn}^{2+}$ ,  $\text{Zn}^{2+}$ , and  $\text{Cu}^{2+}$  have entered into lattice of the hexaferrites. It was reported earlier in the literature that the  $c/a$  ratio can be used to quantify the structure of the hexaferrite [14]. The range of lattice parameters of our samples lies within the expected range from 3.92 to 4.09 Å for M-type hexaferrites.

Download English Version:

<https://daneshyari.com/en/article/1458955>

Download Persian Version:

<https://daneshyari.com/article/1458955>

[Daneshyari.com](https://daneshyari.com)